https://doi.org/10.1016/j.ymssp.2020.106639

Electromagnetic Vibration Absorber for Torsional Vibration in High Speed Rotational Machine

Biao Xiang and Wai on Wong

The Department of Mechanical Engineering, the Hong Kong Polytechnic University,

Kowloon, Hong Kong SAR, China

Abstract

In this article, the vibration absorbing characteristics of electromagnetic (EM) vibration absorber in the rotational machine is studied. The stiffness characteristic and the damping characteristic of an EM vibration absorber are analyzed. The EM vibration absorber realizes its active controllability by tuning its stiffness coefficient and damping coefficient, and then generates the force and torque through controlling the radial tilting. The dynamic equations of rotational machine and EM vibration absorber are established, and their dynamic responses are analyzed. Theoretical analysis results show that the vibration response of rotational machine and its load rotor can be regulated by tuning the stiffness coefficient and the damping coefficient of torque generated by the EM vibration absorber. Experiments are conducted to verify the theoretical analysis result by measuring the displacement deflections of rotational machine at different rotational speeds with different damping coefficients and stiffness coefficients. Therefore, the vibration absorbing ability for the torsional vibration of rotational machine is tunable by regulating the stiffness coefficient and the damping coefficient, and the control range for vibration can cover the whole working frequency of rotational machine. This method is promising to suppress the vibration of the rotational machine with high rotational speed.

Keywords: EM vibration absorber; rotational machine; stiffness coefficient; damping coefficient; vibration response

Nomenclature

J_m	moment of inertia of PMSM rotor	K	stiffness of shaft between PMSM and load
J_l	moment of inertia of load rotor	C	damping of shaft between PMSM and load
T_m	driving torque generated by PMSM	k_a	stiffness of EM vibration absorber
θ_m	torsional angle of PMSM rotor	c_a	damping of EM vibration absorber
θ_l	torsional angle of load rotor	R_-	equivalent reluctance of negative air-gap
N	turn number of winding	R_+	equivalent reluctance of positive air-gap
I_0	bias current of winding	d_0	bias air-gap between stator and PMSM rotor

i	real control current	d	amount of air-gap to be controlled
μ_0	the vacuum permeability	A	cross-sectional area of air-gap
k_w	the amplification coefficient	k_P	regulating coefficient of comprehensive stiffness
k_s	sensitivity of displacement sensor	k_D	regulating coefficient of damping
α	tilting angle around z axis	f_z	force to control tilting around z axis
β	tilting angle around y axis	f_y	force to control tilting around y axis
r	radius of EM vibration absorber	T_z	torque to control tilting around z axis
ω	rotational frequency	T_y	torque to control tilting around y axis
ω_m	natural frequency of PMSM-EM vibration absorber	λ_m	ratio between rotational frequency ω and ω_m
ω_l	natural frequency of shaft between PMSM and load	λ_l	ratio between rotational frequency ω and ω_l
ξ_m	damping coefficient of PMSM-EM vibration absorber	v	ratio of moment of inertia between load and PMSM
ξ_l	damping coefficient of shaft between PMSM and load	l	distance from sensor to center of mass

1. Introduction

For the rotational machinery with the load rotor, the vibration acting on the driven load and the driving motor affect the control precision of whole motor-load system. Therefore, the study on vibration characteristics of the driving motor and the driven load is important to rotational machines such as the high speed motor system [1-5] and the flywheel storage system with a large disc [6, 7].

In order to mitigate the vibration response of the motor-load system, a vibration absorber with negative stiffness and positive stiffness was proposed in [8]. The nonlinear dynamic characteristics of vibration absorber-rotor system were studied, and experimental results showed that the nonlinear negative stiffness of vibration absorber system broadened the control frequency of rotor system. The free vibration of a torsional vibration system with parametric stiffness excitation was discussed, and vibration characteristics of the drive system were investigated in [9]. The results indicated that this kind of drive system had the potential for improving dynamic characteristics of the motor-load system. Vibration isolators with high-static low-dynamic stiffness were proposed to suppress the vibration of rotor with mass eccentricity in [10-13]. The proposed vibration isolator had linear damping and either linear or nonlinear equivalent stiffness. A tunable dynamic vibration absorber consisting of coil spring and magnetic spring [14] was proposed to suppress the vibration due to the rotor's unbalanced eccentricity. Experimental results showed that the proposed vibration absorber was effective for the vibration mitigation of unbalanced rotor system. A torsional vibration isolator

with quasi-zero stiffness was designed to mitigate the torsional vibration of a rotor system, the results indicated that the torsional vibration isolator with quasi-zero stiffness could surpass the linear counterpart [15]. A dual dynamic vibration absorber [16] with two inertia rings connecting the driving side and the driven side of a synchronous motor was proposed to reduce the torsional vibration of synchronous motor. Numerical results showed that the amplitude of transient vibration on the synchronous motor was significantly reduced. A dynamic vibration absorber using viscoelastic material was proposed and tested for the vibration suppression in a rotational machine system [17]. Liu et al. proposed the semi-active dynamic vibration absorber with the magnetorheological elastomer [18] in a propulsion system, and electromagnetic and thermodynamic simulations were carried out to guarantee the structural design. The results showed that the vibration absorption capacity was acceptable although frequency shift of this semi-active vibration absorber was obvious. Moreover, an EM vibration absorber [19, 20] with an EM transducer and an external electrical circuit was designed, experimental results revealed that the proposed EM vibration absorber reduced the maximum displacement deflection of the host structure. An electrorheological vibration absorber was proposed to reduce torsional vibration of a rotor system [21], and it exhibited good performance on vibration suppression. The magnetic actuator was designed to estimate system characteristics and applied the optimal control force to suppress the synchronous vibration, and the effectiveness of the magnetic actuator on a multi-mass rotor system was experimentally verified [22]. A semi-active vibration control technique with smart spring mechanism was dedicated to a rotational machine to suppress the high-amplitude vibration, and the smart spring mechanism used an indirect piezoelectric stack to change the stiffness characteristic of the rotational machine. Moreover, the genetic algorithm was used to optimize the smart spring mechanism, and it effectively reduced vibration amplitude of the rotor at different operating conditions [23]. The damping property of permanent magnetic bearing was studied, and relationship between the restoring torque and radial translation was developed in [24]. The result showed that the restoring torque increased with the radial translational displacement, and it was probably used to suppress the vibration of flywheel rotor.

The dynamic characteristics of a two-mass resonant rotor system were analyzed, and a control method was proposed for vibration suppression of the two-mass resonant rotor system [25, 26]. A PID controller with feedback compensation was designed to regulate the rotational speed, analysis

result indicated that the proposed PID controller had good performance and robustness on the vibration suppression of the two-mass resonant rotor system. Furthermore, a PI controller with model predictive control was proposed for suppressing the torsional vibration in an elastic drive system with shaft torque limitation [27]. The PI controller with model predictive control enhanced the robustness by eliminating the steady-state error. Simulation and experimental results verified that the proposed PI controller with model predictive control was more effective on suppressing the torsional vibration than the PI controller designed by the pole-placement method. Neural network [28, 29] was proposed for the state estimation of the driving system with an elastic joint. The proposed neural network estimator of torsional torque and rotational speed was tested in the closed loop and open loop control systems for reducing the torsional vibration of rotational machine. In literature [30], an adaptive notch filter was used to reject the torsional vibration of the permanent magnet synchronous motor (PMSM), experimental results verified the effectiveness of the proposed adaptive notch filter.

Above all, almost vibration absorbing methods used in the rotational machine are passive, those absorbers can only suppress the vibration with certain frequency, so the control range for vibration frequency is quite limited. Therefore, when the frequency of vibration acting on the rotational machine exceeds the effective range of vibration absorber, those vibration absorbers will be invalid. In addition, some control methods in the active vibration control for rotational machine are focused on the strategy of speed governing, even hard to be implemented in the practical vibration control. Therefore, one kind of vibration absorbing method with wide control range and simple realization is worthy of being studied to improve the working precision of the rotational machine.

In this article, a controllable and tunable EM vibration absorber is proposed to regulate the vibration response of the rotational machine and its load. Considering the variation of rotational speed, the stiffness coefficient and the damping coefficient of EM vibration absorber are tuned to generate corresponding torques. This method is easy to be realized, and the vibration response of rotational machine and its load can be effectively suppressed. Therefore, it provides one wide-range and feasible vibration suppression method for the speed-varying rotational machine.

The introduction about the rotational machine with EM vibration absorber is presented in section 2, and model of force and torque are developed in section 3. The dynamic model of PMSM rotor with EM vibration absorber are studied in section 4, and dynamic responses of PMSM rotor

and load rotor are analyzed in section 5. Finally, in section 6, experimental results are presented to demonstrate effectiveness of the EM vibration absorber on the vibration suppression of PMSM rotor.

2. Structure of PMSM Rotor with EM Vibration Absorber

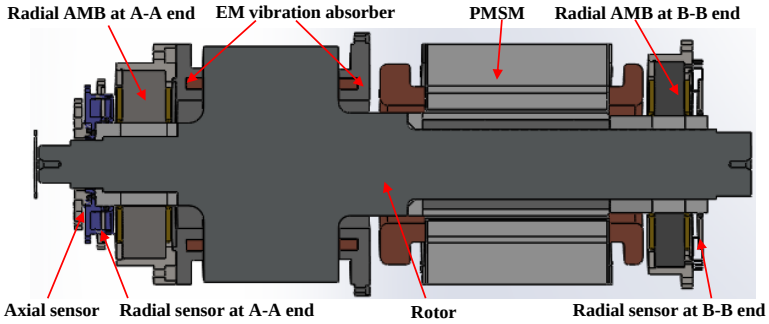

Fig. 1. Structure of the PMSM rotor with EM vibration absorber.

The structure of PMSM rotor and EM vibration absorber is illustrated in Fig. 1. Two pairs of radial active magnetic bearings (AMBs) at the driving end (A-A end and B-B end) generate magnetic forces to make the PMSM rotor stably suspended at the radial equivalent point. The EM vibration absorber mounted at the suspension end is used to regulate the dynamic response of PMSM rotor and load rotor. In addition, displacement sensors at two sides of the driving end can measure the displacement deflections of PMSM rotor in the radial and axial directions. The load rotor is mounted at the rotor shaft of PMSM.

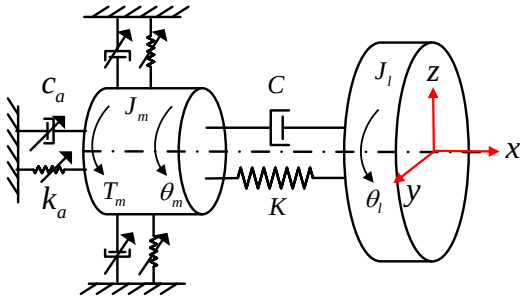

Fig. 2. Simplified model of PMSM rotor with EM vibration absorber.

Based on the structure of PMSM rotor and EM vibration absorber in Fig. 1, the simplified model is shown in Fig. 2. The EM vibration absorber is modelled as a set of tunable spring and damper in axial direction, its stiffness coefficient and damping coefficient can be adjusted based on the displacement feedback. Therefore, the simplified model is similar to the two-mass resonant rotational system [31-33], the difference is that the control range of PMSM rotor-EM vibration absorber system can be regulated based on the feedback control system, but the control frequency of two-mass

resonant rotational system is a fixed frequency. Assuming the moment of inertia of PMSM rotor is J_m, and the moment of inertia of load rotor is J_l, T_m is the driving torque generated by PMSM rotor. θ_m is the torsional angle of PMSM rotor. K is the stiffness of connection shaft between PMSM rotor and load rotor, C is the damping of connecting shaft between PMSM rotor and load rotor, θ_l is the torsional angle of load rotor. k_a is the stiffness of EM vibration absorber, c_a is the damping of EM vibration absorber.

3. Model of EM Vibration Absorber

3.1. Force Model of EM Vibration Absorber

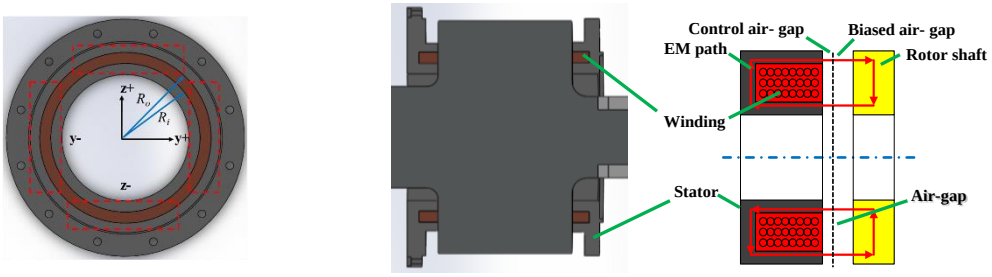

(a) (b)

Fig. 3. Model of EM vibration absorber, (a) stator and winding, (b) cross-sectional view and simplified model.

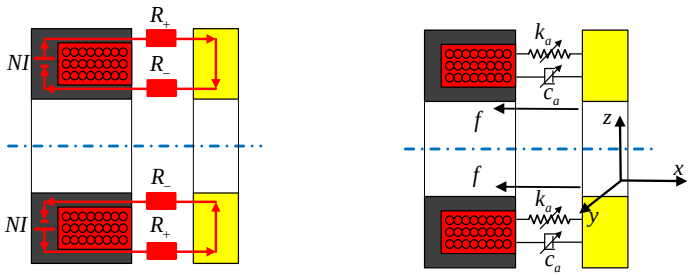

(a) (b)

Fig. 4. Equivalent model of EM vibration absorber, (a) equivalent magnet path, (b) equivalent force model.

The structure of EM vibration absorber is illustrated in Fig. 3. There are four sub-windings in one side of the rotor shaft, and the windings in z+ and z- direction are in series connection. An air-gap exists between the stator and the rotor part of EM vibration absorber, and the air-gap is divided into the bias air-gap and the control air-gap in the practical engineering. In addition, the bias air-gap is much larger than the control air-gap. The winding of EM vibration absorber regulate the control flux to generate magnetic force based on the displacement feedback.

As illustrated in Fig. 4(a), the magnet flux generated by the winding in z+ and z- direction passes through the stator, the air-gap and the rotor, and it returns back to the stator of EM vibration absorber. The total magnet motive force generated by the EM vibration absorber is written as

$$F=N\cdot(I_0+i) \tag{1}$$

where N is the turn number of winding, I_0 is the bias current of winding, i is the real control current. R_- is the equivalent reluctance of air-gap in negative direction, R_+ is the equivalent reluctance of air-gap in positive direction, and the total reluctance of air-gap is expressed as following

$$R=R_+ +R_- =\frac{2(d_0+d)}{\mu_0 A} \tag{2}$$

where d_0 is the bias air-gap between the stator and the rotor of PMSM, d is the amount of air-gap to be controlled, μ_0 is the vacuum permeability, A is the cross-sectional area of air-gap. The magnet flux is

$$\Phi=\frac{F}{R}=\frac{N(I_0+i)\cdot\mu_0 A}{2(d_0+d)} \tag{3}$$

The magnetic force generated by the EM vibration absorber is the attractive force to realize the active control. The magnetic force generated by the EM vibration absorber is written as

$$f=\frac{\Phi^2}{\mu_0 A}=\frac{N^2\mu_0 A}{4}\cdot\frac{(I_0+i)^2}{(d_0+d)^2} \tag{4}$$

The EM force coefficient is defined as

$$k_{amb}=\frac{N^2\mu_0 A}{4} \tag{5}$$

If $d=0$ and $i=0$, the current stiffness and the displacement stiffness is written respectively as

$$k_i=\frac{\partial f}{\partial i}=2k_{amb}\cdot\frac{I_0+i}{(d_0+d)^2}\approx 2k_{amb}\cdot\frac{I_0}{d_0^2}\Bigg|\begin{matrix} i=0 \\ d=0 \end{matrix} \tag{6}$$

$$k_d=\frac{\partial f}{\partial d}=-2k_{amb}\cdot\frac{(I_0+i)^2}{(d_0+d)^3}\approx -2k_{amb}\cdot\frac{I_0^2}{d_0^3}\Bigg|\begin{matrix} i=0 \\ d=0 \end{matrix} \tag{7}$$

So the magnetic force can be expressed into

$$f=k_i i+k_d d \tag{8}$$

3.2. Feedback Model of EM Vibration Absorber

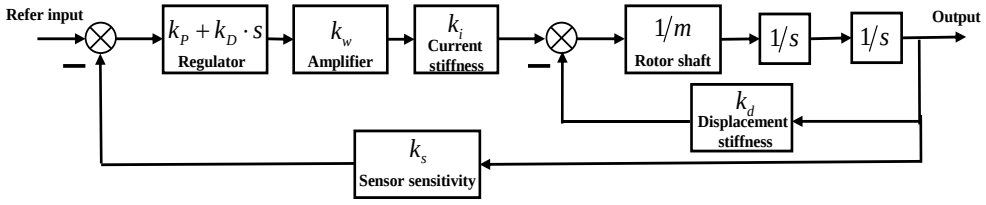

Fig. 5. Feedback control system of EM vibration absorber.

The feedback control scheme of EM vibration absorber system is illustrated in Fig. 5. The

displacement deflections between the rotor and the stator are measured by displacement sensors. The difference between measured displacement and reference displacement is used to tune the stiffness coefficient and the damping coefficient of EM vibration absorber. The negative displacement stiffness is used to regulate the comprehensive stiffness of EM vibration absorber. Finally, the transfer function of feedback control can be expressed as

$$G(s)=\frac{k_i k_w k_P + k_i k_w k_D s}{ms^2 + k_i k_w k_s k_D s + k_i k_w k_s k_P - k_d} \tag{9}$$

The comprehensive stiffness of EM vibration absorber is

$$k = k_i k_w k_s k_P - k_d = k_{iws} k_P - k_d \tag{10}$$

where k_w is the amplification coefficient, k_s is the sensitivity of displacement sensor, and k_P is the regulating coefficient of comprehensive stiffness. In addition, the damping coefficient of EM vibration absorber can be achieved as in the following,

$$c = k_{iws} k_D \tag{11}$$

where k_D is the regulating coefficient of damping.

Therefore, the equivalent dynamic performance of EM vibration absorber may be modelled by the tunable spring-damper model as shown in Fig. 4(b). The comprehensive stiffness of EM vibration absorber can be regulated by the regulating coefficient k_P, and the damping of EM vibration absorber can be tuned by the regulating coefficient k_D.

3.3. Torque Model of EM Vibration Absorber

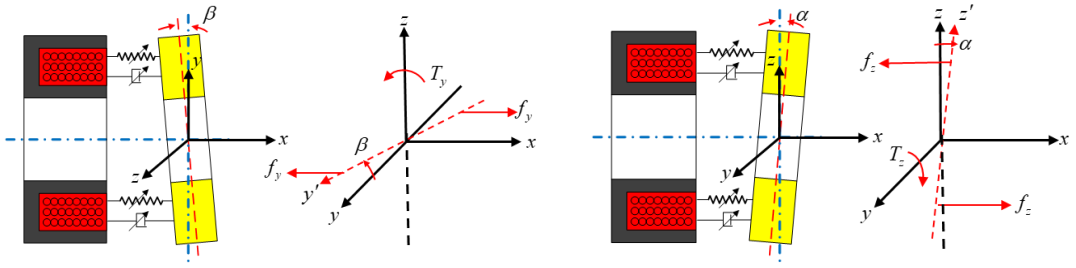

(a) (b)

Fig. 6. Torque model of EM vibration absorber, (a) torque around y axis, (b) torque around z axis.

The torque model of EM vibration absorber is shown in Fig. 6, the PMSM rotor tilts around y axis, and the tilting angle is β. Furthermore, as illustrated in Fig. 6(a), the EM vibration absorber generate force f_y to control the tilting around y axis when the tilting happens to rotor part, and the torque is T_y. Similarly, the tilting of PMSM rotor around z axis is illustrated in Fig. 6(b), and the

tilting angle around z axis is α. Therefore, the force f_z generated by EM vibration absorber will push the PMSM rotor back to the equilibrium point, and the torque is T_z. R is the radius of EM vibration absorber. Moreover, torques around y axis and z axis are, respectively,

$$T_z = f_z \cdot R = k_z \cdot \alpha + c_z \cdot \dot{\alpha} \tag{12}$$

$$T_y = f_y \cdot R = k_y \cdot \beta + c_y \cdot \dot{\beta} \tag{13}$$

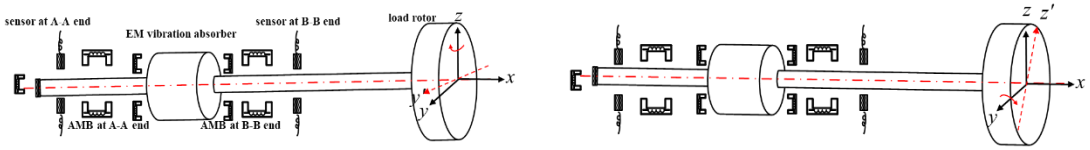

(a) (b)

Fig. 7. Tilting mode of PMSM rotor, (a) tilting around y axis, (b) tilting around z axis.

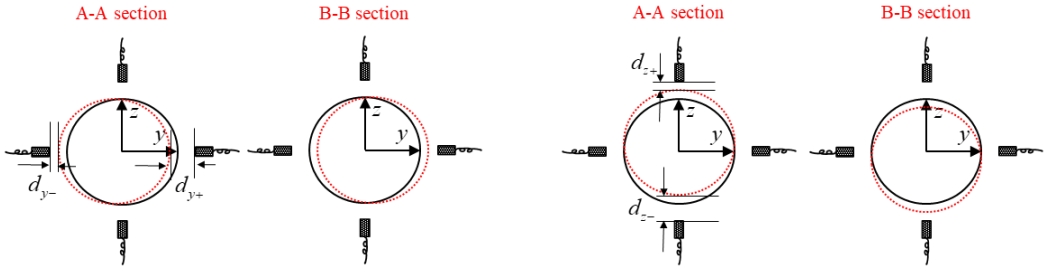

(a) (b)

Fig. 8. Displacement deflection of PMSM rotor, (a) titling around y axis, (b) tilting around z axis.

When the PMSM rotor tilts at β about the y axis as shown in Fig 6(a), the detection point of the displacement sensor moves away from the sensor in the y+ direction as shown in Fig. 7(a). Therefore, the displacement d_{y+} in Fig. 8(a) increases, and the displacement d_{y-} decreases. Similarly, when the PMSM rotor tilts at α about the z axis in Fig 6(b), the detection point of the displacement sensor moves closer to the sensor in the z+ direction as shown in Fig. 8(b). Therefore, the displacement d_{z+} decreases, and the displacement d_{z-} increases. The distance from the displacement sensor to center of mass is l. As tilting angle α and β are fairly small values, they can be rewritten as

$$\beta \approx \sin\beta = \frac{d_{z+} - d_{z-}}{2l} \tag{14}$$

$$\alpha \approx \sin\alpha = \frac{d_{y+} - d_{y-}}{2l} \tag{15}$$

Furthermore, we define k_a=k_y =k_z and c_a=c_y =c_z. Using Eq.(10) and Eq.(11), the tilting stiffness and the damping of EM vibration absorber can be written into

$$k_a = (k_{iws} k_P - k_d) lr \tag{16}$$

$$c_a = k_{iws} k_D lr \tag{17}$$

4. Modeling of PMSM Rotor and EM Vibration Absorber System

4.1. Modeling with Damping and Stiffness of EM Vibration Absorber

Based on the model of PMSM rotor-EM vibration absorber system in Fig. 2, equations of motion of PMSM rotor and load rotor are expressed respectively as

$$J_m\ddot{\theta}_m = T_m + k_a\theta_m + c_a\dot{\theta}_m - K\left(\theta_m - \theta_l\right) - C\left(\dot{\theta}_m - \dot{\theta}_l\right) \tag{18}$$

$$J_l\ddot{\theta}_l = K\left(\theta_m - \theta_l\right) + C\left(\dot{\theta}_m - \dot{\theta}_l\right) \tag{19}$$

Transfer functions of PMSM rotor and load rotor are written respectively as

$$G_m(s) = \frac{\Theta_m(s)}{T_m(s)} = \frac{J_l s^2 + Cs + K}{\left[J_m s^2 + \left(C - c_a\right)s + \left(K - k_a\right)\right]\left(J_l s^2 + Cs + K\right) - \left(Cs + K\right)^2} \tag{20}$$

$$G_l(s) = \frac{\Theta_l(s)}{T_m(s)} = \frac{Cs + K}{\left[J_m s^2 + \left(C - c_a\right)s + \left(K - k_a\right)\right]\left(J_l s^2 + Cs + K\right) - \left(Cs + K\right)^2} \tag{21}$$

Furthermore, the dimensionless frequency response functions are written as

$$G_m(j\omega) = \frac{\lambda_l^2\left(1 - \lambda_l^2 + 2j\xi_l\lambda_l\right)}{\lambda_l^2\left(1 - \lambda_l^2 + 2j\xi_l\lambda_l\right)\left(1 - \lambda_m^2 + 2j\xi_m\lambda_m\right) - \nu\lambda_m^2\left(1 + 2j\xi_l\lambda_l\right)^2} \tag{22}$$

$$G_l(j\omega) = \frac{\lambda_l^2\left(1 + 2j\xi_l\lambda_l\right)}{\lambda_l^2\left(1 - \lambda_l^2 + 2j\xi_l\lambda_l\right)\left(1 - \lambda_m^2 + 2j\xi_m\lambda_m\right) - \nu\lambda_m^2\left(1 + 2j\xi_l\lambda_l\right)^2} \tag{23}$$

where $\omega_m = \sqrt{\frac{K - k_a}{J_m}}$ is the natural frequency of PMSM rotor-EM vibration absorber. $\omega_l = \sqrt{\frac{K}{J_l}}$ is the natural frequency of connecting shaft between PMSM rotor and load rotor. $\lambda_m = \frac{\omega}{\omega_m}$ is the ratio between rotational frequency ω and ω_m. $\lambda_l = \frac{\omega}{\omega_l}$ is the ratio between rotational frequency ω and ω_l. $\xi_m = \frac{C - c_a}{2J_m\omega_m}$ is the damping coefficient of PMSM rotor-EM vibration absorber. $\xi_l = \frac{C}{2J_l\omega_l}$ is the damping coefficient of connecting shaft between PMSM rotor and load rotor. $\nu = \frac{J_l}{J_m}$ is the ratio of moment of inertia between load rotor and PMSM rotor.

In order to simplify the dimensionless frequency response functions, Eq.(22) and Eq.(23) are rewritten into

$$G_m(j\omega) = \frac{c + jd}{a + jb} \tag{24}$$

$$G_l(j\omega) = \frac{e + jf}{a + jb} \tag{25}$$

where

$$\begin{cases} a = \lambda_l^2\left(1-\lambda_l^2\right)\left(1-\lambda_m^2\right)-4\xi_l\xi_m\lambda_l^3\lambda_m-\nu\lambda_m^2\left(1-4\xi_l^2\lambda_l^2\right) \\ b = 2\xi_l\lambda_l^3\left(1-\lambda_m^2\right)+2\xi_m\lambda_m\lambda_l^2\left(1-\lambda_m^2\right)-4\nu\xi_l\lambda_l\lambda_m^2 \\ c = \lambda_l\left(1-\lambda_l^2\right) \\ d = 2\xi_l\lambda_l^3 \\ e = \lambda_l^2 \\ f = 2\xi_l\lambda_l^3 \end{cases} \tag{26}$$

The response magnitudes of PMSM rotor and load rotor are obtained as following,

$$\begin{cases} A_m = \left|G_m\left(j\omega\right)\right| = \dfrac{\sqrt{c^2+d^2}}{\sqrt{a^2+b^2}} \\ A_l = \left|G_l\left(j\omega\right)\right| = \dfrac{\sqrt{e^2+f^2}}{\sqrt{a^2+b^2}} \end{cases} \tag{27}$$

4.2. Modeling with Stiffness of EM Vibration Absorber

If the damping coefficient c_a of the connecting shaft of PMSM rotor-EM vibration absorber is not considered in the dynamics function of PMSM rotor-load system, the vibration absorbing model of EM vibration absorber is simplified into a pure proof mass mounted at end of PMSM rotor. Therefore, Eq.(22) and Eq.(23) are rewritten as

$$G_m'\left(j\omega\right) = \frac{\lambda_l^2\left(1-\lambda_l^2+2j\xi_l\lambda_l\right)}{\lambda_l^2\left(1-\lambda_l^2+2j\xi_l\lambda_l\right)\left(1-\lambda_m^2+2j\xi_m'\lambda_m\right)-\nu\lambda_m^2\left(1+2j\xi_l\lambda_l\right)^2} \tag{28}$$

$$G_l'\left(j\omega\right) = \frac{\lambda_l^2\left(1+2j\xi_l\lambda_l\right)}{\lambda_l^2\left(1-\lambda_l^2+2j\xi_l\lambda_l\right)\left(1-\lambda_m^2+2j\xi_m'\lambda_m\right)-\nu\lambda_m^2\left(1+2j\xi_l\lambda_l\right)^2} \tag{29}$$

where $\xi_m' = \dfrac{C}{2J_m\omega_m}$ is the damping coefficient of PMSM rotor-EM vibration absorber. Compared with Eq.(22) and Eq.(23), the damping coefficient increases and the natural frequency remains the same because the vibration absorbing model of EM vibration absorber is simplified into a pure proof mass.

4.3. Modeling with Damping of EM Vibration Absorber

On the other hand, if the stiffness coefficient k_a of PMSM rotor-EM vibration absorber is not considered, the vibration absorbing method of EM vibration absorber is reduced into a pure damper, so Eq.(22) and Eq.(23) can be rewritten as

$$G_m''(j\omega)=\frac{\lambda_l^2\left(1-\lambda_l^2\right)}{\lambda_l^2\left(1-\lambda_l^2\right)\left(1-\left(\lambda_m''\right)^2+2j\xi_m''\lambda_m''\right)-\nu\left(\lambda_m''\right)^2\left(1+2j\xi_l\lambda_l\right)^2} \tag{30}$$

$$G_l''(j\omega)=\frac{\lambda_l^2}{\lambda_l^2\left(1-\lambda_l^2\right)\left(1-\left(\lambda_m''\right)^2+2j\xi_m''\lambda_m''\right)-\nu\left(\lambda_m''\right)^2\left(1+2j\xi_l\lambda_l\right)^2} \tag{31}$$

where $\omega_m''=\sqrt{\frac{K}{J_m}}$ is the second natural frequency of PMSM rotor-EM vibration absorber. $\xi_m''=\frac{C-c_a}{2J_m\omega_m''}$ is the second damping coefficient of PMSM rotor-EM vibration absorber, and $\lambda_m''=\frac{\omega}{\omega_m''}$ is the second frequency ratio. Compared with Eq.(22) and Eq.(23), the natural frequency increases and damping coefficient decreases when the vibration absorbing model of EM vibration absorber is simplified into a pure damper model.

4.4. Modeling without Stiffness and Damping of EM Vibration Absorber

Furthermore, if both the stiffness coefficient k_a and the damping coefficient c_a of EM vibration absorber are not considered, Eq.(22) and Eq.(23) can be simplified as

$$G_m''(j\omega)=\frac{\lambda_l^2\left(1-\lambda_l^2\right)}{\lambda_l^2\left(1-\lambda_l^2\right)\left(1-\left(\lambda_m'''\right)^2+2j\xi_m'''\lambda_m'''\right)-\nu\left(\lambda_m'''\right)^2\left(1+2j\xi_l\lambda_l\right)^2} \tag{32}$$

$$G_l''(j\omega)=\frac{\lambda_l^2}{\lambda_l^2\left(1-\lambda_l^2\right)\left(1-\left(\lambda_m'''\right)^2+2j\xi_m'''\lambda_m'''\right)-\nu\left(\lambda_m'''\right)^2\left(1+2j\xi_l\lambda_l\right)^2} \tag{33}$$

where $\omega_m'''=\sqrt{\frac{K}{J_m}}$ is the third natural frequency of PMSM rotor-EM vibration absorber. $\xi_m'''=\frac{C}{2J_m\omega_m'''}$ is the third damping coefficient of PMSM rotor-EM vibration absorber, and $\lambda_m'''=\frac{\omega}{\omega_m'''}$ is the third frequency ratio.

5. Numerical Simulation

5.1. Dynamic Response of Load Rotor

Based on the dynamic model in Eq.(22) and Eq.(23), the relationship between dynamic characteristics of PMSM rotor and load rotor are studied. Firstly, the effect of damping coefficient c_a of EM vibration absorber on the dynamic response of load rotor are plotted in Fig. 9(a). Compared with the dynamic response of load rotor with the damping coefficient of EM vibration absorber, the response peak of load rotor occurs when the damping coefficient of EM vibration absorber is not considered. Obviously, the response magnitude of load rotor with the damping coefficient of EM

vibration absorber is smaller than the response magnitude without the damping coefficient. In addition, the relationship between the response magnitude of load rotor and the damping coefficient of EM vibration absorber is illustrated in Fig. 9(b), the result shows that the response magnitude of load rotor decreases with the damping coefficient of EM vibration absorber. Therefore, the response magnitude of load rotor can be suppressed by increasing the damping coefficient of EM vibration absorber.

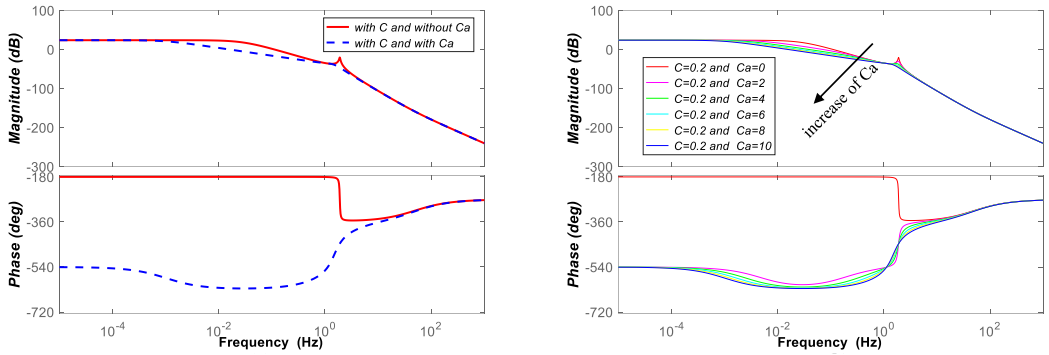

(a) (b)

Fig. 9. Response of load rotor with damping of EM vibration absorber, (a) comparison, (b) response with damping.

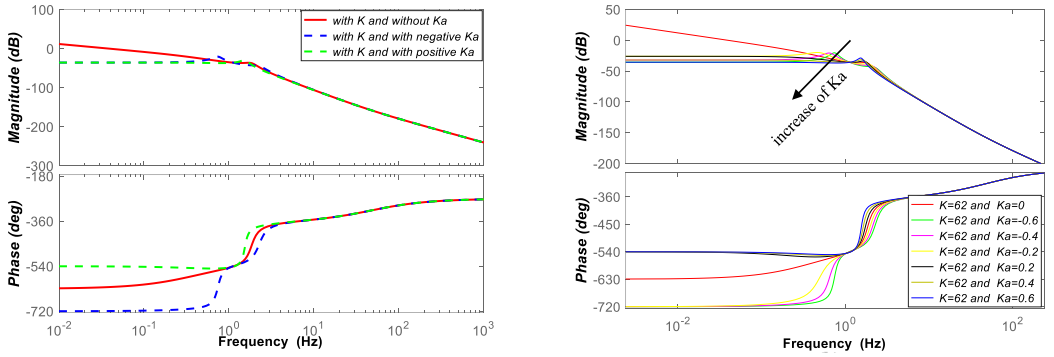

(a) (b)

Fig. 10. Response of load rotor with stiffness of EM vibration absorber, (a) comparison, (b) response with stiffness.

Secondly, the effect of the comprehensive stiffness k_a of EM vibration absorber is analyzed. When the comprehensive stiffness of EM vibration absorber is negative value, the dynamic response of load rotor is shown by the blue line in Fig. 10(a). There are two response peaks at different frequencies in the spectrum, and the response magnitude at low frequency is greater than that at high frequency. If the comprehensive stiffness of EM vibration absorber is tuned into positive value, the dynamic response of load rotor is shown by the green line in Fig. 10(a). Compared with the dynamic response of load rotor with negative comprehensive stiffness of EM vibration absorber, the positive comprehensive stiffness of EM vibration absorber can avoid the vibration peak at low frequency.

Moreover, the relationship between the dynamic response of load rotor and the comprehensive stiffness of EM vibration absorber is shown in Fig. 10(b), the response magnitude of load rotor decreases with the comprehensive stiffness of EM vibration absorber. Therefore, the dynamic response of load rotor decreases with the comprehensive stiffness coefficient of EM vibration absorber.

Finally, the dynamic response of load rotor without using EM vibration absorber is plotted in Fig. 11(a). The response magnitude is relatively higher than that in Fig. 10(a) with the presence of comprehensive stiffness of EM vibration absorber. The comparison shows that the comprehensive stiffness and the damping coefficient of EM vibration absorber system are useful to suppress the vibration response of load rotor.

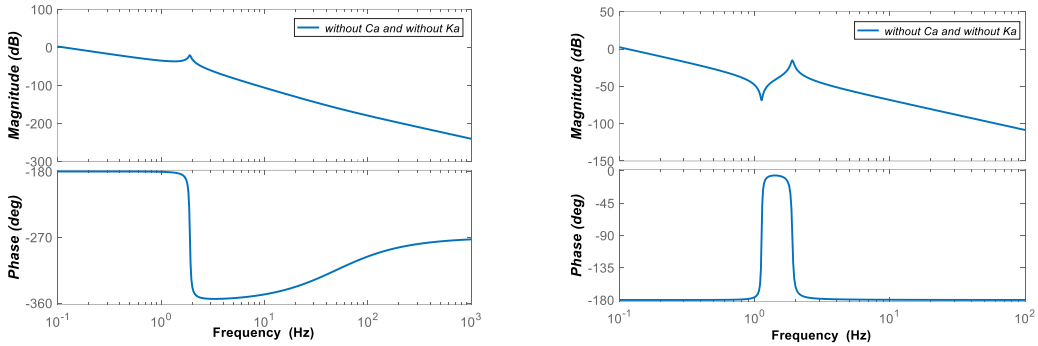

(a) (b)

Fig. 11. (a) Response of load rotor without EM vibration absorber, (b) Response of PMSM rotor without EM vibration absorber.

5.2. Dynamic Response of PMSM rotor

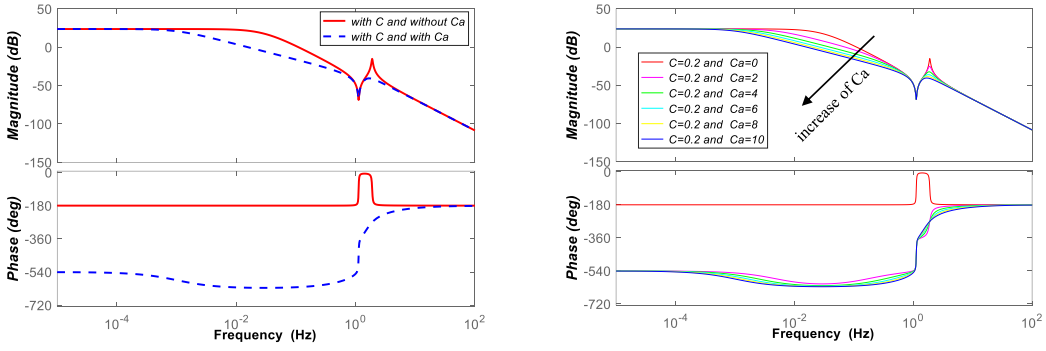

(a) (b)

Fig. 12. (a) Response of PMSM rotor with damping of EM vibration absorber, (b) response with damping.

When the damping coefficient c_a of EM vibration absorber is not applied, the dynamic response of PMSM rotor is illustrated by the red line in Fig. 12(a). When the damping coefficient c_a of EM

vibration absorber is applied, the response of PMSM rotor is shown by the blue line in Fig. 12(a), the response magnitude of PMSM rotor is less than that without the damping of EM vibration absorber. So the damping coefficient of EM vibration absorber can affect the dynamic response of PMSM rotor too. In addition, the relationship between the dynamic response of PMSM rotor and the damping coefficient of EM vibration absorber is shown in Fig. 12(b). The response magnitude of PMSM rotor declines with the damping coefficient of EM vibration absorber. Therefore, the damping coefficient of EM vibration absorber can mitigate the vibration response of PMSM rotor.

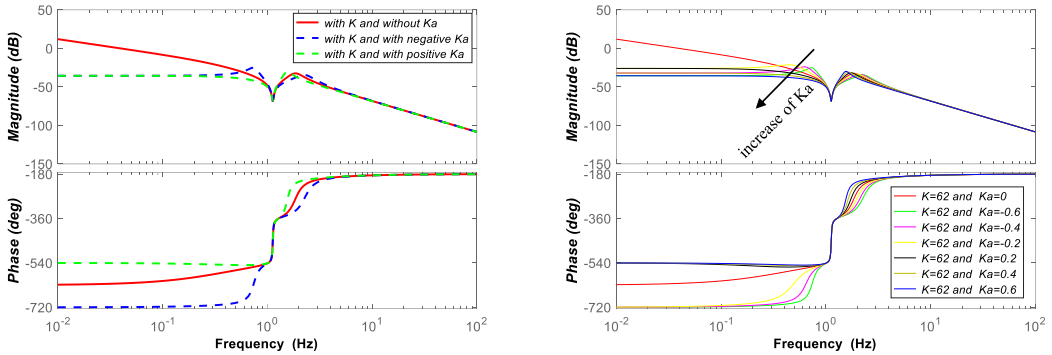

(a) (b)

Fig. 13. (a) Response of PMSM rotor with stiffness of EM vibration absorber, (b) response with stiffness.

Moreover, as illustrated in Fig. 13(a), when the comprehensive stiffness of EM vibration absorber is tuned to a negative value, the dynamic response of PMSM rotor is indicated by the blue line, and the dynamic response of PMSM rotor with positive comprehensive stiffness is shown by the green line. The response magnitude of PMSM rotor with negative comprehensive stiffness is greater than that of PMSM rotor with positive comprehensive stiffness. The relationship between the dynamic response of PMSM rotor and the comprehensive stiffness of EM vibration absorber is illustrated in Fig. 13(b). The response magnitude of PMSM rotor decreases with comprehensive stiffness of EM vibration absorber. Therefore, the positive comprehensive stiffness of EM vibration absorber can mitigate the vibration response of PMSM rotor too.

Finally, the dynamic response of PMSM rotor without using EM vibration absorber is shown in Fig. 11(b). The response magnitude of PMSM rotor without using EM vibration absorber is greater than that in Fig. 12 and Fig. 13. The damping coefficient and the stiffness coefficient of EM vibration absorber are useful to mitigate the vibration response of PMSM rotor.

6. Experimental Verification

6.1. Experimental Setup

Experiments were conducted to verify the effect of EM vibration absorber on the dynamic response of PMSM rotor. The whole experimental system is shown in Fig. 14. The experimental setup is composed of four parts: the control unit, the PMSM system, the measurement system and the monitoring system. The control unit is based on a DSP chip and a FPGA chip, a 12-bit A/D convertor chip is used to the communication between the host computer and the control unit. The PWM amplifier is used to drive the winding of EM vibration absorber. The measurement system is consisted of displacement sensors and the data acquisition (DAQ) system. The displacement deflection between the rotor and the stator of PMSM is measured by the displacement sensors. The displacement signal is transmitted to the monitoring system by the A/D convertor and the DAQ system. The system parameters of whole experimental setup are listed in TABLE. I

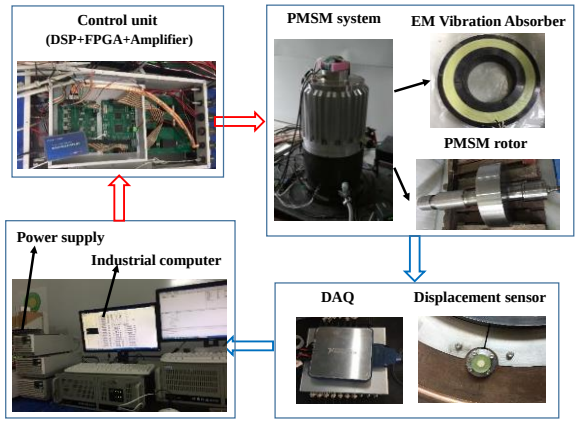

Fig. 14. Experimental setup.

TABLE. I. PARAMETERS of EXPERIMENTAL SETUP.

Parameter	*Value*	*Unit*
Inertia of moment of PMSM rotor	J_m=0.67	kg·m^2
Inertia of moment of load rotor	J_l=1.24	kg·m^2
Stiffness of connecting shaft of PMSM-load	K=62	Nm/rad
Damping of connecting shaft of PMSM-load	C=0.012	Nm/rad/s
Current stiffness of EM vibration absorber	k_i=1750	N/A
Displacement stiffness of EM vibration absorber	k_d=-550	N/mm
Distance from radial sensor to center of mass	l=476	mm
Radius of EM vibration absorber	R=225	mm
Angle stiffness of EM vibration absorber	-161.5	Nm/rad
Current torque stiffness of EM vibration absorber	2.3	Nm/A
Amplification coefficient	k_w=0.2	A/V
Sensitivity of displacement sensor	k_s=3.3	V/mm

6.2. Force and Torque of EM Vibration Absorber

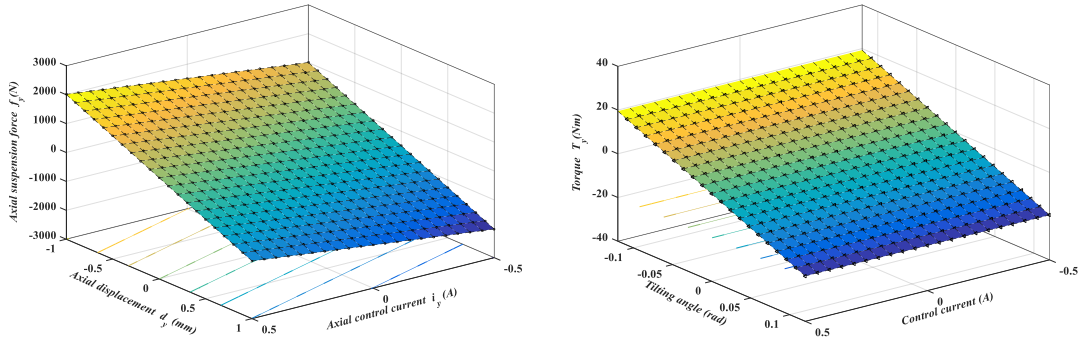

(a) (b)

Fig. 15. The force and torque of EM vibration absorber, (a) force, (b) torque.

The relationships amongst the force, the control current and the control displacement are shown in Fig. 15(a). The force is positively linear to the control current, but it is inversely proportional to the control displacement. In detail, the current stiffness is 1750N/A, and the displacement stiffness is -550N/mm. The torque generated by EM vibration absorber is shown in Fig. 15(b). The torque has linear relationships with control displacement and control current within the vicinity of the equilibrium point. The angle stiffness of torque is -161.5Nm/rad, and the current stiffness of torque is 2.3Nm/A. Therefore, the torque generated by EM vibration absorber is tunable by regulating the control current based on the feedback control.

6.3. Relationship between Vibration of PMSM Rotor and Damping of EM Vibration Absorber

The maximum displacement obviation of PMSM rotor deflecting from the radial equilibrium point is the evaluation index for the vibration response, greater the maximum displacement obviation of PMSM rotor is, greater the vibration response. The dynamic displacements of PMSM rotor are measured at different statuses of EM vibration absorber in Fig. 16. Firstly, the maximum dynamic displacements of PMSM rotor at different speeds are plotted in Fig. 17(a), and the maximum displacement deflections of PMSM rotor with different damping coefficients are listed in TABLE. II. When the rotational speed of PMSM rotor is at 2000rpm and the damping coefficient of EM vibration absorber sets at 2, the maximum displacement deflection of PMSM rotor is 0.0156mm. The maximum displacement deflection decreases to 0.0078mm when the damping coefficient is 8 and the rotational speed of PMSM rotor remains unchanged. Furthermore, when the rotational speed of PMSM rotor increases to 8000rpm, the maximum displacement deflection of PMSM rotor is about

0.0161mm when the damping coefficient of EM vibration absorber is 2, and it declines to 0.0135mm when the damping coefficient increases to 8.

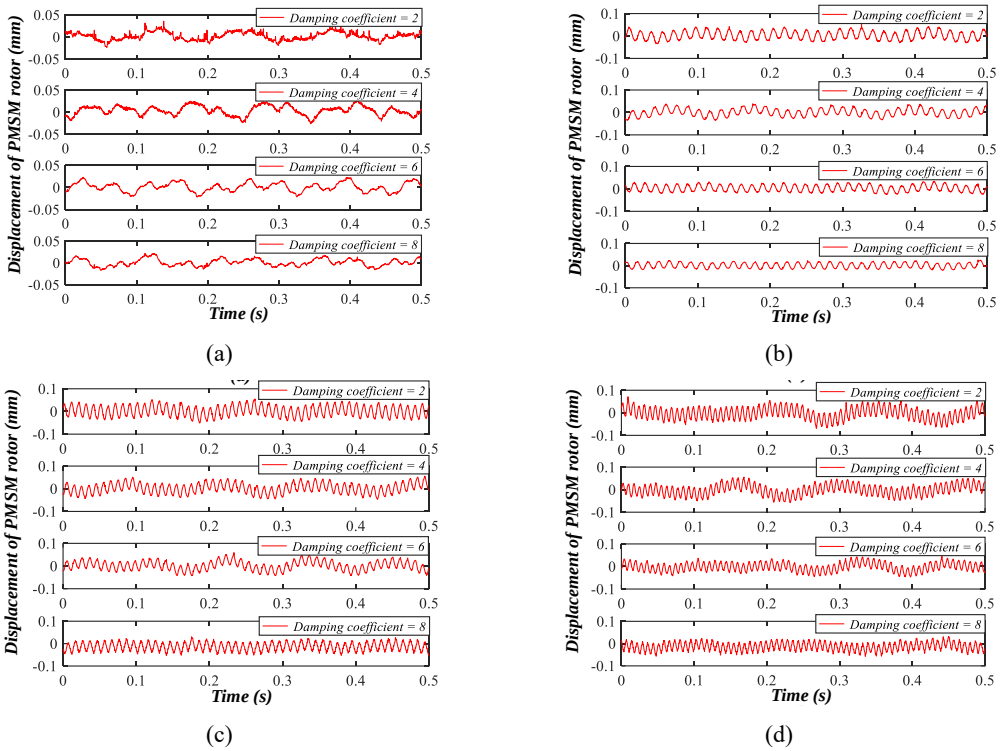

Fig. 16. Displacement with damping coefficient, (a) speed=2000rpm, (b) speed=4000rpm, (c) speed=6000rpm, (d) speed=8000rpm.

TABLE. II. MAXIMUM DISPLACEMENT DEFLECTION WITH DAMPING COEFFICIENT

Damping coefficient	Maximum displacement deflection (mm)			
	speed=2000rpm	speed=4000rpm	speed=6000rpm	speed=8000rpm
1	0.0160	0.0164	0.0168	0.0169
2	0.0156	0.0150	0.0162	0.0161
3	0.0154	0.0144	0.0149	0.0155
4	0.0152	0.0135	0.0143	0.0152
5	0.0139	0.0125	0.0139	0.0145
6	0.0110	0.0112	0.0137	0.0140
7	0.0103	0.0111	0.0131	0.0138
8	0.0078	0.0105	0.0126	0.0135
9	0.0075	0.0103	0.0123	0.0129
10	0.0073	0.0102	0.0114	0.0113

Moreover, based on dynamic displacements of PMSM rotor in Fig. 16, response magnitudes of PMSM rotor at different rotational speeds with different damping coefficients of EM vibration absorber are illustrated in Fig. 18. In Fig. 18(a), the response magnitude of PMSM rotor is -108dB when the damping coefficient sets at 2, and it decreases to -141dB when the damping coefficient is

8. When the rotational speed of PMSM rotor is 8000rpm in Fig. 18(d), the response magnitude is -73dB when the damping coefficient is 2, and it decreases to -79dB when the damping coefficient increases to 8. Consequently, the maximum displacement deflection of PMSM rotor is intensified alongside the rotational speed of PMSM rotor, and it decreases with the increase of damping coefficient of EM vibration absorber.

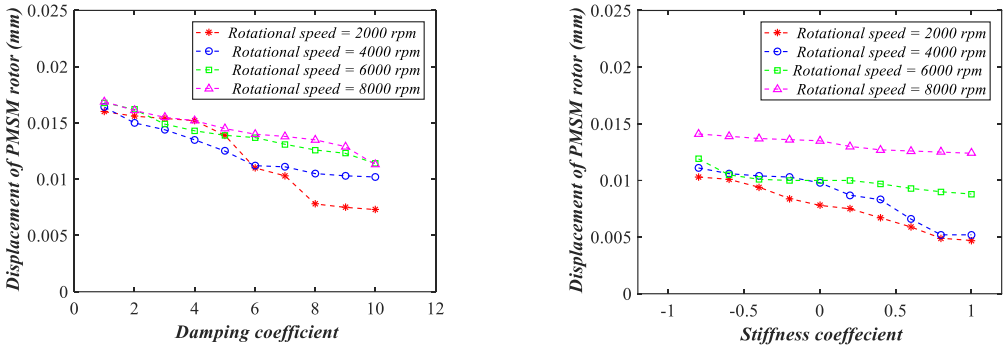

Fig. 17. Maximum displacement deflection, (a) damping coefficient, (b) stiffness coefficient.

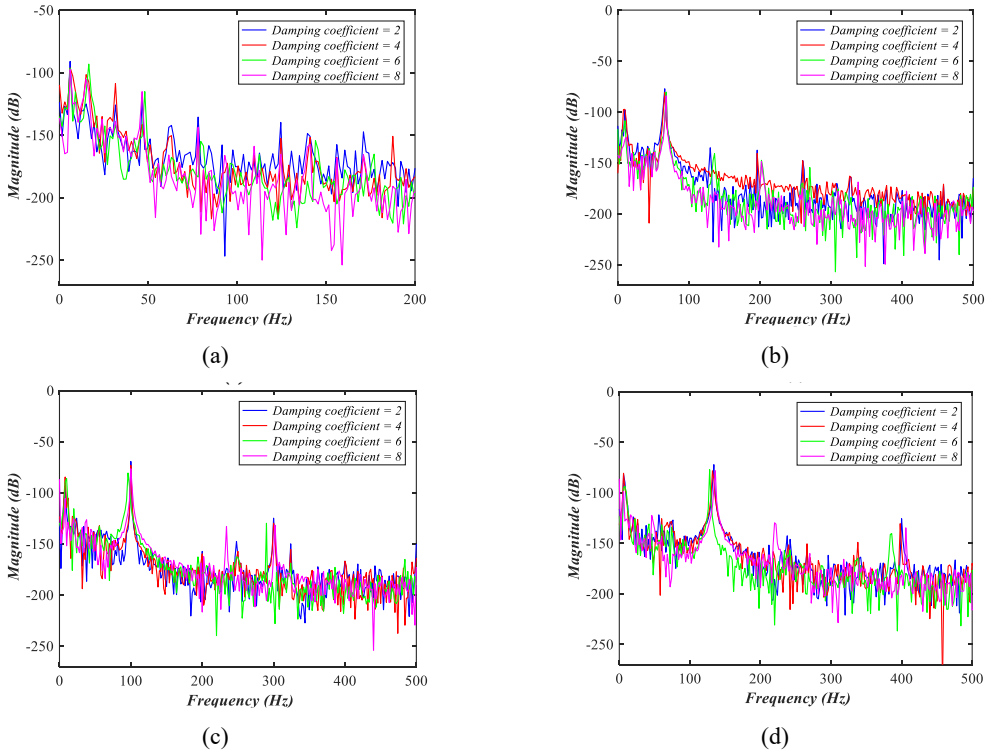

Fig. 18. Response magnitude with damping coefficient, (a) speed=2000rpm, (b) speed=4000rpm, (c) speed=6000rpm, (d) speed=8000rpm.

6.4. Relationship between Vibration of PMSM Rotor and Stiffness of EM Vibration Absorber

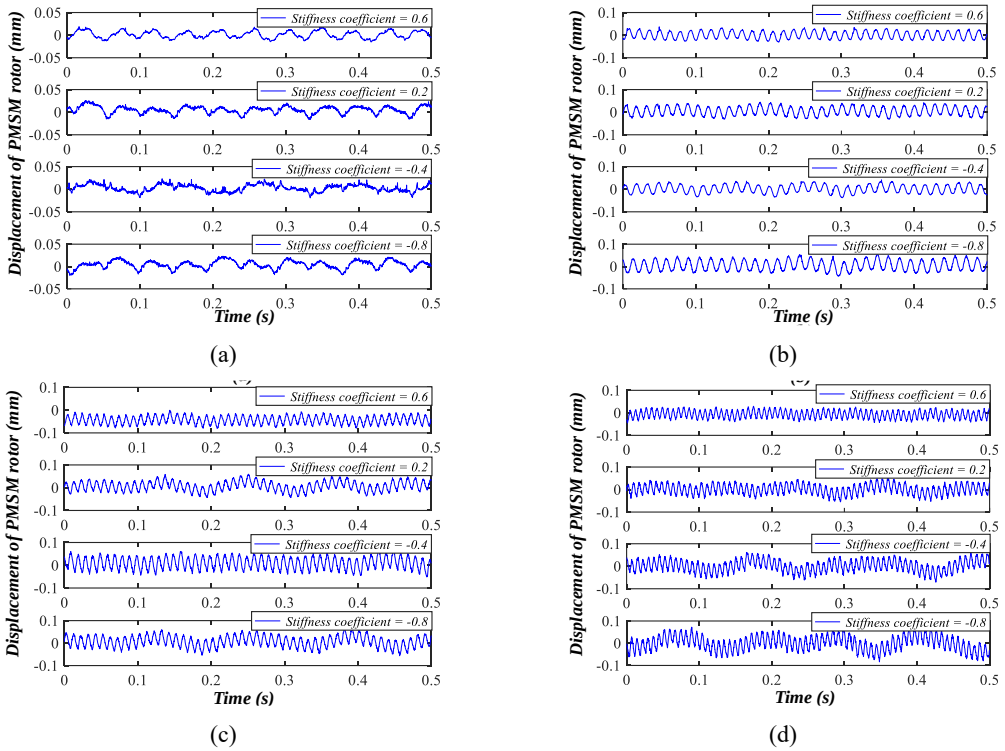

Fig. 19. Displacement with stiffness coefficient, (a) speed=2000rpm, (b) speed=4000rpm, (c) speed=6000rpm, (d) speed=8000rpm.

In addition, dynamic displacements of PMSM rotor with different stiffness coefficients of EM vibration absorber are plotted in Fig. 19. The maximum displacement deflections of PMSM rotor are listed in

TABLE. III and plotted in Fig. 17(b). When the rotational speed of PMSM rotor is 2000rpm, the maximum displacement deflection of PMSM rotor is 0.0101mm when the stiffness coefficient of EM vibration absorber is -0.8, and the maximum displacement deflection decreases to 0.0049mm when the stiffness coefficient is 0.6. When the PMSM rotor works at 8000rpm, the maximum displacement deflection is 0.0139mm when the stiffness coefficient of EM vibration absorber is -0.8, and the maximum displacement deflection is reduced to 0.0125mm if the stiffness coefficient is 0.6.

In addition, response magnitudes of PMSM rotor at 2000rpm are shown in Fig. 20(a). When the stiffness coefficient of EM vibration absorber is -0.8, the response magnitude is -113dB, and it decreases to -148dB when the stiffness coefficient is 0.6. Furthermore, response magnitudes of PMSM rotor with rotational speed increases to 8000rpm are shown in Fig. 20(d). The response magnitude of PMSM rotor is -70dB when the stiffness coefficient is -0.8, and it decreases to -78dB

when the stiffness coefficient is 0.6.

TABLE. III. MAXIMUM DISPLACEMENT DEFLECTION WITH STIFFNESS COEFFICIENT.

Stiffness coefficient	Maximum displacement deflection (mm)			
	speed=2000rpm	speed=4000rpm	speed=6000rpm	speed=8000rpm
0.8	0.0047	0.0052	0.0088	0.0124
0.6	0.0049	0.0052	0.0090	0.0125
0.4	0.0059	0.0066	0.0093	0.0126
0.2	0.0067	0.0083	0.0097	0.0127
0	0.0075	0.0087	0.0100	0.0130
-0.2	0.0078	0.0098	0.0100	0.0135
-0.4	0.0084	0.0103	0.0100	0.0136
-0.6	0.0094	0.0104	0.0101	0.0137
-0.8	0.0101	0.0106	0.0105	0.0139
-1	0.0103	0.0111	0.0119	0.0141

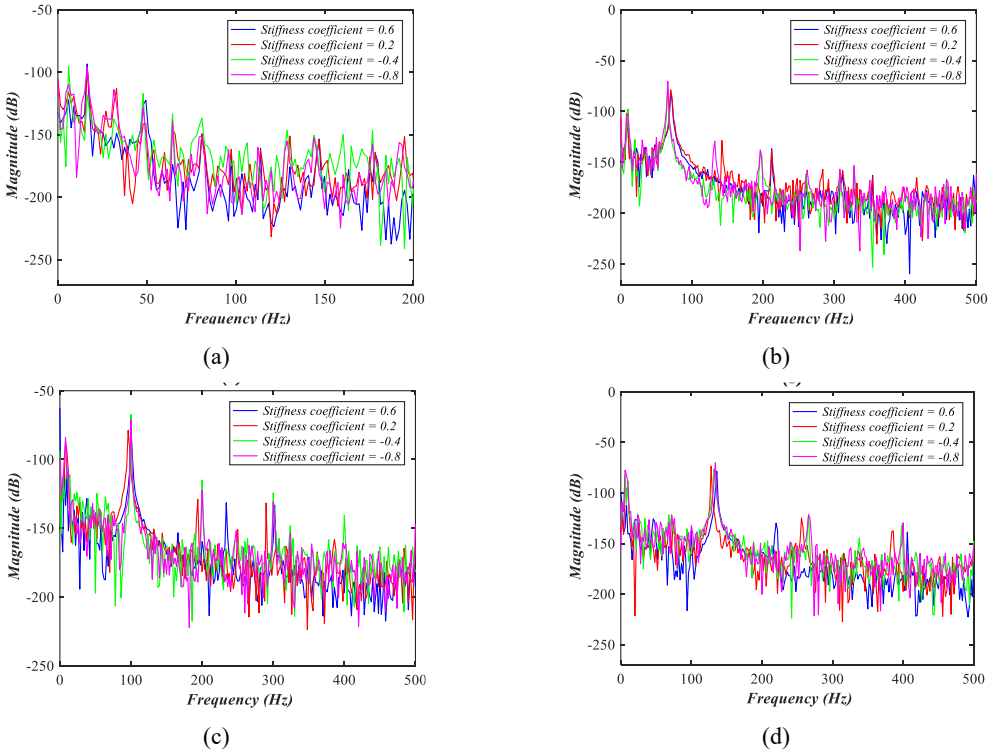

Fig. 20. Response magnitude with stiffness coefficient, (a) speed=2000rpm, (b) speed=4000rpm, (c) speed=6000rpm, (d) speed=8000rpm.

Above all, dynamic displacements of PMSM rotor show that the vibration magnitude of PMSM rotor increases with the rotational speed. More importantly, the experimental results also indicates that the vibration response of PMSM rotor can be suppressed by regulating the stiffness coefficient and the damping coefficient of EM vibration absorber. Moreover, for the EM vibration absorber, the

effective range of vibration suppression is not only at fixed rotational frequency, but also cover the whole working frequency of PMSM rotor.

6.5. Vibration Response of PMSM Rotor with Accelerating

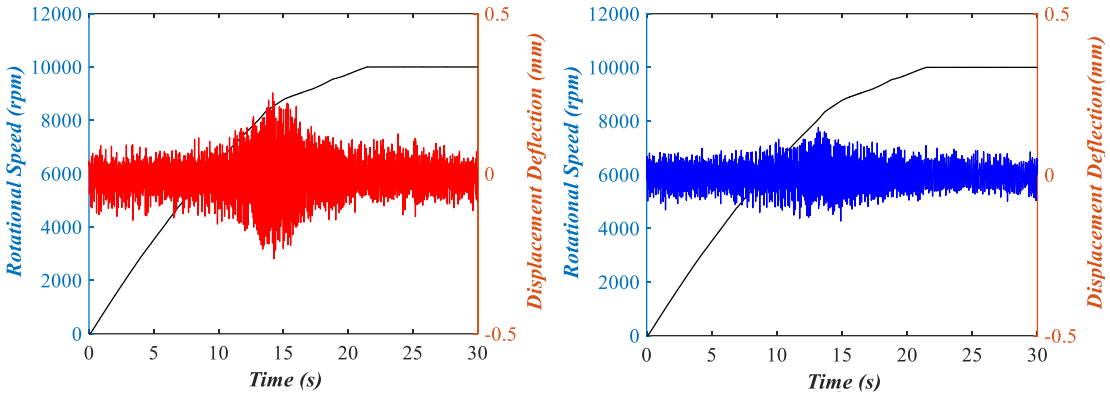

(a) (b)

Fig. 21. Displacement of PMSM rotor with accelerating, (a) without EM vibration absorber, (b) with EM vibration absorber.

Finally, the dynamic displacements of PMSM rotor when it is accelerated to the rated speed 10000rpm are measured and plotted in Fig. 21, and the maximum displacement deflection of PMSM rotor is the evaluation index of vibration response. With the condition that the damping coefficient sets at 8 and the displacement stiffness sets at 0.6, when the EM vibration absorber is not applied, the dynamic displacements is shown in Fig. 21(a), and the maximum displacement deflection of PMSM rotor is 0.5179mm. When the EM vibration absorber is used, the maximum displacement deflection of PMSM rotor is declined to 0.2912mm in Fig. 21(b), the relative reduction is about 43.8%. Therefore, the EM vibration absorber is effective on suppressing the vibration response of PMSM rotor during the procedure of accelerating.

7. Conclusion

The EM vibration absorber mounted on the axial suspension end of PMSM rotor-load system is used to regulate the vibration response of PMSM rotor. The controllability of EM vibration absorber is verified by the modelling of the force and torque. The comprehensive stiffness and damping coefficient of EM vibration absorber are tunable based on the displacement feedback of PMSM rotor. Furthermore, the damping coefficient and the stiffness coefficient of EM vibration absorber can effectively suppress the vibration response of PMSM rotor. Finally, experiments results confirm that the maximum displacement deflection of PMSM rotor increases with the rotational frequency, and

decreases with stiffness coefficient and also the damping coefficient of EM vibration absorber. Therefore, the EM vibration absorber can be used to suppress the vibration response of high-speed motor with load rotor, and the effective range of vibration suppression is broadened by the EM vibration absorber based on the displacement feedback.

Acknowledgements

This work was supported by The Hong Kong Polytechnic University [grant number CRG RUMT16900506r].

References

[1] S. Park, W. Kim, S.-I. Kim, A numerical prediction model for vibration and noise of axial flux motors, IEEE Transactions on Industrial Electronics, 61 (2014) 5757-5762.

[2] W. Sun, Y. Li, J. Huang, N. Zhang, Vibration effect and control of In-Wheel Switched Reluctance Motor for electric vehicle, Journal of Sound and Vibration, 338 (2015) 105-120.

[3] H.-J. Shin, J.-Y. Choi, H.-I. Park, S.-M. Jang, Vibration analysis and measurements through prediction of electromagnetic vibration sources of permanent magnet synchronous motor based on analytical magnetic field calculations, IEEE Transactions on Magnetics, 48 (2012) 4216-4219.

[4] S.M. Castano, B. Bilgin, E. Fairall, A. Emadi, Acoustic noise analysis of a high-speed high-power switched reluctance machine: Frame effects, IEEE Transactions on Energy Conversion, 31 (2016) 69-77.

[5] J. Licari, C.E. Ugalde-Loo, J.B. Ekanayake, N. Jenkins, Damping of torsional vibrations in a variable-speed wind turbine, IEEE transactions on energy conversion, 28 (2013) 172-180.

[6] T. Asami, O. Nishihara, A.M. Baz, Analytical solutions to H∞ and H2 optimization of dynamic vibration absorbers attached to damped linear systems, Journal of vibration and acoustics, 124 (2002) 284-295.

[7] X. Chang, Y. Li, W. Zhang, N. Wang, W. Xue, Active disturbance rejection control for a flywheel energy storage system, IEEE Transactions on Industrial Electronics, 62 (2015) 991-1001.

[8] H. Yao, Z. Chen, B. Wen, Dynamic vibration absorber with negative stiffness for rotor system, Shock and Vibration, 2016 (2016).

[9] H. Ecker, T. Pumhössel, Vibration suppression and energy transfer by parametric excitation in drive systems, Proceedings of the Institution of Mechanical Engineers, Part C: Journal of Mechanical Engineering Science, 226 (2012) 2000-2014.

[10] A. Abbasi, S. Khadem, S. Bab, M. Friswell, Vibration control of a rotor supported by journal bearings and an asymmetric high-static low-dynamic stiffness suspension, Nonlinear Dynamics, 85 (2016) 525-545.

[11] A. Abbasi, S. Khadem, S. Bab, Vibration control of a continuous rotating shaft employing high-static low-dynamic stiffness isolators, Journal of Vibration and Control, 24 (2018) 760-783.

[12] H. Navazi, M. Hojjati, Nonlinear vibrations and stability analysis of a rotor on high-static-low-dynamic-stiffness supports using method of multiple scales, Aerospace Science and Technology, 63 (2017) 259-265.

[13] S.H. Kia, H. Henao, G.-A. Capolino, Torsional vibration effects on induction machine current and torque signatures in gearbox-based electromechanical system, IEEE Transactions on Industrial Electronics, 56 (2009) 4689-4699.

[14] H. Yao, T. Wang, B. Wen, B. Qiu, A tunable dynamic vibration absorber for unbalanced rotor system, Journal of Mechanical Science and Technology, 32 (2018) 1519-1528.
[15] J. Zhou, D. Xu, S. Bishop, A torsion quasi-zero stiffness vibration isolator, Journal of Sound and Vibration, 338 (2015) 121-133.
[16] B. Al-Bedoor, K. Moustafa, K. Al-Hussain, Dual dynamic absorber for the torsional vibrations of synchronous motor-driven compressors, Journal of sound and vibration, 220 (1999) 729-748.
[17] F. Doubrawa Filho, M. Luersen, C. Bavastri, Optimal design of viscoelastic vibration absorbers for rotating systems, Journal of Vibration and Control, 17 (2011) 699-710.
[18] G. Liu, K. Lu, D. Zou, Z. Xie, Z. Rao, N. Ta, Development of a semi-active dynamic vibration absorber for longitudinal vibration of propulsion shaft system based on magnetorheological elastomer, Smart Materials and Structures, 26 (2017) 075009.
[19] A. Gonzalez-Buelga, L. Clare, S. Neild, S. Burrow, D. Inman, An electromagnetic vibration absorber with harvesting and tuning capabilities, Structural Control and Health Monitoring, 22 (2015) 1359-1372.
[20] M. Sasaki, T. Sugiura, Vibration reduction of rotor supported by superconducting magnetic bearing utilizing electromagnetic shunt damper, IEEE Transactions on Applied Superconductivity, 26 (2016) 1-4.
[21] Y. Sun, M. Thomas, Control of torsional rotor vibrations using an electrorheological fluid dynamic absorber, Journal of Vibration and Control, 17 (2011) 1253-1264.
[22] R.S. Srinivas, R. Tiwari, C. Kannababu, Application of active magnetic bearings in flexible rotordynamic systems–A state-of-the-art review, Mechanical Systems and Signal Processing, 106 (2018) 537-572.
[23] A.A. Cavalini, T.V. Galavotti, T.S. Morais, E.H. Koroishi, V. Steffen, Vibration attenuation in rotating machines using smart spring mechanism, Mathematical Problems in Engineering, 2011 (2011).
[24] C. Liu, G. Liu, Equivalent damping control of radial twist motion for permanent magnetic bearings based on radial position variation, IEEE Transactions on Industrial Electronics, 62 (2015) 6417-6427.
[25] G. Shahgholian, P. Shafaghi, Simple analytical and robust controller design for two-mass resonant system, in: Computer and Electrical Engineering, 2009. ICCEE'09. Second International Conference on, IEEE, 2009, pp. 245-248.
[26] G. Shahgholian, Modeling and simulation of a two-mass resonant system with speed controller, International Journal of Information and Electronics Engineering, 3 (2013) 448.
[27] C. Wang, M. Yang, W. Zheng, J. Long, D. Xu, Vibration suppression with shaft torque limitation using explicit MPC-PI switching control in elastic drive systems, IEEE Transactions on Industrial Electronics, 62 (2015) 6855-6867.
[28] T. Orlowska-Kowalska, K. Szabat, Neural-network application for mechanical variables estimation of a two-mass drive system, IEEE Transactions on Industrial Electronics, 54 (2007) 1352-1364.
[29] Y. Amer, A. El-Sayed, F. El-Bahrawy, Torsional vibration reduction for rolling mill's main drive system via negative velocity feedback under parametric excitation, Journal of Mechanical Science and Technology, 29 (2015) 1581-1589.
[30] D.-H. Lee, J. Lee, J.-W. Ahn, Mechanical vibration reduction control of two-mass permanent magnet synchronous motor using adaptive notch filter with fast Fourier transform analysis, IET electric power applications, 6 (2012) 455-461.
[31] G. Shahgholian, P. Shafaghi, Simple analytical and robust controller design for two-mass resonant system, in: 2009 Second International Conference on Computer and Electrical Engineering, IEEE, 2009, pp. 245-248.

[32] A. Ghaemmaghami, R. Kianoush, X.X. Yuan, Numerical modeling of dynamic behavior of annular tuned liquid dampers for applications in wind towers, Computer-Aided Civil and Infrastructure Engineering, 28 (2013) 38-51.
[33] K. Szabat, T. Orlowska-Kowalska, Vibration suppression in a two-mass drive system using PI speed controller and additional feedbacks—Comparative study, IEEE Transactions on Industrial Electronics, 54 (2007) 1193-1206.